

Effects of short-range correlations on nuclear symmetry energy within a modified Gogny-Hartree-Fock energy density functional approach

Bao-Jun Cai*^{1,2,3} and Bao-An Li^{†1}

¹*Department of Physics and Astronomy, Texas A&M University-Commerce, Commerce, TX 75429-3011, USA*

²*Department of Physics, Shanghai University, Shanghai 200444, China*

³*Department of Physics and Astronomy and Shanghai Key Laboratory for Particle Physics and Cosmology, Shanghai Jiao Tong University, Shanghai 200240, China*

(Dated: December 3, 2024)

Within a modified Gogny-Hartree-Fock (GHF) energy density functional (EDF) encapsulating the nucleon-nucleon short-range correlations (SRC)-induced high momentum tail (HMT) in the single-nucleon momentum distribution, we investigate effects of the SRC-induced HMT on the density dependence of nuclear symmetry energy $E_{\text{sym}}(\rho)$. After re-optimizing the modified GHF-EDF by reproducing the same empirical properties of symmetric nuclear matter (SNM), symmetry energy $E_{\text{sym}}(\rho_0)$ and its slope L as well as major features of nucleon optical potential at saturation density ρ_0 , the $E_{\text{sym}}(\rho)$ is found to decrease at both sub-saturation and supra-saturation densities, leading to a reduced curvature K_{sym} of $E_{\text{sym}}(\rho)$ and subsequently a smaller coefficient K_τ for the isospin-dependence of nuclear incompressibility in better agreement with its experimental value. Astrophysical implications of the SRC-modified symmetry energy are also discussed. In particular, the SRC effects are found to decrease the proton fraction as well as the core-crust transition density and pressure in neutron stars at β equilibrium. Moreover, the SRC-modified EOS and single-nucleon potentials can be used in future transport model simulations of heavy-ion collisions to investigate SRC effects in dense neutron-rich matter in terrestrial laboratories.

PACS numbers: 21.65.Ef, 24.10.Ht, 21.65.Cd

Introduction: The Gogny-Hartree-Fock (GHF) nuclear energy density functional (EDF) has been playing an important role in nuclear physics because of its special feature that the finite-range part of the Gogny interaction [1] leads to a momentum dependent single-particle potential through the exchange term in the potential energy density within Hartree-Fock calculations. In particular, the resulting single-nucleon potential and equation of state (EOS) of nuclear matter have been widely used in understanding many interesting phenomena in heavy-ion collisions from low to relativistic energies, see, e.g., refs. [2–7] as well as in studying various properties of stellar matter and neutron stars, see, e.g., refs. [8–12]. Earlier GHF-EDFs for symmetric nuclear matter (SNM) were extended in recent years to isospin-asymmetric nuclear matter (ANM) by incorporating the isospin dependence, see, e.g., refs. [13–15]. Applying them in transport model simulations of nuclear reactions involving neutron-rich nuclei, see, e.g., refs. [16–20], have allowed us to learn many interesting new physics regarding both the role of isospin degree of freedom and the elusive density dependence of nuclear symmetry energy $E_{\text{sym}}(\rho)$. The latter is critically important for both nuclear physics and astrophysics but still poorly known especially at supra-saturation densities, see, e.g., reviews in ref. [21]. In this work, using an isospin-dependent single-nucleon momentum distribution with a high momentum tail (HMT) in ANM at zero temperature constrained by recent electron-nucleus scattering data and a new regulating function within the GHF-EDF, we study effects of the HMT induced

by short-range nucleon-nucleon correlations (SRC) on the $E_{\text{sym}}(\rho)$ and their astrophysical implications. It is found that the HMT reduces the $E_{\text{sym}}(\rho)$ at both sub-saturation and supra-saturation densities, leading to an isospin-dependent incompressibility K_τ in better agreement with the experimental data. Implications of the SRC-modified $E_{\text{sym}}(\rho)$ on the cooling mechanisms as well as the density and pressure at the core-crust transition point in neutron stars are also discussed.

Single-Nucleon Momentum Distribution Function Encapsulating SRC-induced high momentum tail: It is well known that the SRC leads to a high (low) momentum tail (depletion) in the single-nucleon momentum distribution function denoted by $n_{\mathbf{k}}^J$ above (below) the nucleon Fermi surface in cold nucleonic matter [22–27]. Significant efforts have been made in recent years both theoretically and experimentally to constrain the isospin-dependent parameters characterizing the SRC-modified $n_{\mathbf{k}}^J$ in neutron-rich nucleonic matter [28–33]. In particular, it has been found via analyzing electron-nucleus scattering data that the percentage of nucleons in the HMT above the Fermi surface is as high as about $28\% \pm 4\%$ in SNM but decreases gradually to about only $1\% \sim 2\%$ in pure neutron matter (PNM) [30, 31]. On the other hand, the predicted size of the HMT still depends on the model and interaction used. For instance, the self-consistent Green’s function (SCGF) theory using the AV18 interaction predicts a $11\% \sim 13\%$ HMT for SNM at saturation density and a $4\% \sim 5\%$ HMT in PNM [34].

For completeness and the ease of the following discussions, we first briefly describe the SRC-modified single-nucleon momentum distribution function encapsulating a HMT constrained by the available SRC data that we shall use in this work. The single-nucleon momentum distribution function in

*Email: bjcai87@gmail.com

[†]Corresponding author: Bao-An.Li@tamuc.edu

cold ANM has the following form [35–38]

$$n_{\mathbf{k}}^J(\rho, \delta) = \begin{cases} \Delta_J, & 0 < |\mathbf{k}| < k_F^J, \\ C_J (k_F^J/|\mathbf{k}|)^4, & k_F^J < |\mathbf{k}| < \phi_J k_F^J. \end{cases} \quad (1)$$

Here, $k_F^J = k_F(1 + \tau_3^J \delta)^{1/3}$ is the Fermi momentum where $k_F = (3\pi^2 \rho/2)^{1/3}$, $\tau_3^n = +1$ and $\tau_3^p = -1$, respectively, and $\delta = (\rho_n - \rho_p)/(\rho_n + \rho_p)$ is the isospin asymmetry. The above form of $n_{\mathbf{k}}^J(\rho, \delta)$ was found consistent with the well-known predictions of microscopic nuclear many-body theories [22–25] and the recent experimental findings [28–32]. This form of $n_{\mathbf{k}}^J(\rho, \delta)$ has been applied to address several issues regarding the HMT effects recently in both nuclear physics and astrophysics [35–42].

The parameters Δ_J , C_J and ϕ_J are assumed to depend linearly on δ based on predictions of microscopic many-body theories [34, 43, 44] $Y_J = Y_0(1 + Y_1 \tau_3^J \delta)$ [35]. The amplitude C_J and high-momentum cutoff coefficient ϕ_J determine the fraction of nucleons in the HMT via

$$x_J^{\text{HMT}} = 3C_J(1 - \phi_J^{-1}). \quad (2)$$

Moreover, the normalization condition between the density ρ_J and the distribution $n_{\mathbf{k}}^J$, i.e., $[2/(2\pi)^3] \int_0^\infty n_{\mathbf{k}}^J(\rho, \delta) d\mathbf{k} = \rho_J = (k_F^J)^3/3\pi^2$ requires that only two of the three parameters, i.e., C_J , ϕ_J and Δ_J , are independent. Here we choose the first two as independent and determine the Δ_J by

$$\Delta_J = 1 - 3C_J(1 - \phi_J^{-1}) = 1 - x_J^{\text{HMT}}. \quad (3)$$

Meanwhile, the adopted $C/|\mathbf{k}|^4$ shape of the HMT both for SNM and PNM is strongly supported by recent studies both theoretically and experimentally [30, 45]. It is interesting to point out that the $|\mathbf{k}|^{-4}$ form of the HMT is also found in Bose system theoretically [46–48] and experimentally [49, 50], indicating a very general feature of the HMT. For comparisons, we use two HMT parameter sets. The $n_{\mathbf{k}}^J$ adopting a 28% HMT in SNM and a 1.5% HMT in PNM [30, 31] is abbreviated as the HMT-exp set, and that adopting a 12% HMT in SNM and a 4% HMT in PNM [34] as the HMT-SCGF set [38]. Moreover, the model using a step function for the $n_{\mathbf{k}}^J$ is denoted as the free Fermi gas (FFG) set as a reference. As discussed in more details in ref. [38], the HMT parameters in the HMT-exp (HMT-SCGF) parameter set are $\phi_0 \approx 2.38$ ($\phi_0 \approx 1.49$), $\phi_1 \approx -0.56$ ($\phi_1 \approx -0.25$), $C_0 \approx 0.161$ ($C_0 \approx 0.121$), and $C_1 \approx -0.25$ ($C_1 \approx -0.01$), respectively.

Incorporating single-nucleon momentum distributions with HMTs in Gogny Hartree-Fock energy density functionals: In most studies of heavy-ion collisions using transport models, one parameterizes the EDFs and determine their parameters by reproducing empirical properties of SNM at the saturation density ρ_0 , a selected value of symmetry energy $E_{\text{sym}}(\rho_0)$ and its slope $L \equiv [3\rho dE_{\text{sym}}(\rho)/d\rho]_{\rho_0}$ as well as main features of nucleon optical potentials extracted from analyzing nucleon-nucleus scatterings, such as the isosclar and isovector nucleon effective masses and their asymptotic values at high momenta at ρ_0 , etc., see, e.g., ref. [17] for detailed discussions. For example, using a modified Gogny-type momentum-dependent

interaction (MDI) first proposed by Das *et al* [14, 51], a modified GHF-EDF in terms of the average energy per nucleon $E(\rho, \delta)$ in ANM at density ρ and isospin asymmetry δ can be written as

$$E(\rho, \delta) = \sum_{J=n,p} \frac{1}{\rho_J} \int_0^\infty \frac{\mathbf{k}^2}{2M} n_{\mathbf{k}}^J(\rho, \delta) d\mathbf{k} + \frac{A_\ell(\rho_p^2 + \rho_n^2)}{2\rho\rho_0} + \frac{A_u\rho_p\rho_n}{\rho\rho_0} + \frac{B}{\sigma+1} \left(\frac{\rho}{\rho_0}\right)^\sigma (1 - x\delta^2) + \sum_{J,J'} \frac{C_{J,J'}}{\rho\rho_0} \int d\mathbf{k} d\mathbf{k}' f_J(\mathbf{r}, \mathbf{k}) f_{J'}(\mathbf{r}, \mathbf{k}') \Omega(\mathbf{k}, \mathbf{k}'). \quad (4)$$

The first term is the kinetic energy while the three terms in the second line are the usual zero-range 2-body and effective 3-body contributions characterized by their strength parameters A_ℓ , A_u and B as well as the density dependence σ of the 3-body force [14, 51]

$$A_\ell = A_\ell^0 + \frac{2xB}{1+\sigma}, \quad A_u = A_u^0 - \frac{2xB}{1+\sigma} \quad (5)$$

where x controls the competition between the isosinglet and isotriplet 2-body interactions, and it affects only the slope L but not the $E_{\text{sym}}(\rho_0)$ be design [14]. The last term in Eq. (4) is the contribution to the EOS from the finite-range 2-body interactions characterized by the strength parameter $C_{J,J} \equiv C_\ell$ for like and $C_{J,\bar{J}} \equiv C_u$ for unlike nucleon pairs, respectively, using the notations $\bar{n} = p$ and $\bar{p} = n$. The $f_J(\mathbf{r}, \mathbf{k})$ and $n_{\mathbf{k}}^J(\rho, \delta)$ are the nucleon phase space distribution function and momentum distribution function, respectively. In equilibrated nuclear matter at zero temperature, they are related by

$$f_J(\mathbf{r}, \mathbf{k}) = \frac{2}{h^3} n_{\mathbf{k}}^J(\rho, \delta) = \frac{1}{4\pi^3} n_{\mathbf{k}}^J(\rho, \delta), \quad \hbar = 1. \quad (6)$$

For example, in the FFG, $n_{\mathbf{k}}^J = \Theta(k_F^J - |\mathbf{k}|)$ with Θ the standard step function, then $f_J(\mathbf{r}, \mathbf{k}) = (1/4\pi^3)\Theta(k_F^J - |\mathbf{k}|)$.

The regulating function $\Omega(\mathbf{k}, \mathbf{k}')$ [2, 14] originating from the meson exchange theory of nuclear force normally has the form of

$$\Omega(\mathbf{k}, \mathbf{k}') = \left[1 + \left(\frac{\mathbf{k} - \mathbf{k}'}{\Lambda} \right)^2 \right]^{-1} \quad (7)$$

where \mathbf{k} and \mathbf{k}' are the momenta of two interacting nucleons and Λ is a parameter regulating the momentum dependence of the single-particle potential. For applications to SNM, it is usually determined by fixing the nucleon isosclar effective mass at the Fermi surface to an empirical value [2, 14]. The single-nucleon potential corresponding to Eq. (4) is given by

$$U_J(\rho, \delta, |\mathbf{k}|) = \frac{A_\ell \rho_J}{\rho_0} + \frac{A_u \rho_{\bar{J}}}{\rho_0} + B \left(\frac{\rho}{\rho_0} \right)^\sigma (1 - x\delta^2) - 4x\tau_3^J \frac{B}{\sigma+1} \frac{\rho^{\sigma-1}}{\rho_0^\sigma} \delta \rho_{\bar{J}} + \sum_{J'} \frac{2C_{J,J'}}{\rho_0} \int d\mathbf{k}' f_{J'}(\mathbf{r}, \mathbf{k}') \Omega(\mathbf{k}, \mathbf{k}'). \quad (8)$$

In applying the above formalisms to transport model simulations of nuclear reactions, the $f_J(\mathbf{r}, \mathbf{k})$ and $n_{\mathbf{k}}^J(\rho, \delta)$ are calculated self-consistently from solving dynamically the coupled Boltzmann-Uehling-Uhlenbeck (BUU) transport or molecular dynamics equations for quasi-nucleons [52, 53]. While in studying thermal properties of hot nuclei or stellar matter in thermal equilibrium, the Fermi-Dirac distributions at finite temperatures are used.

Traditionally, one writes the EDF as a sum of kinetic EOS of FFG plus several potential terms. Before making any applications, the model parameters of the EDFs are normally fixed by using step functions for the $f_J(\mathbf{r}, \mathbf{k})$ and $n_{\mathbf{k}}^J(\rho, \delta)$ as in a FFG at zero temperature in reproducing properties of nuclei or nuclear matter in their ground states. In reality, however, since all nucleons interact with each other in nuclear medium, they naturally become quasi-nucleons. The normal practice of optimizing the EDFs puts all effects of interactions into the potential part of the EDF thus ignores interaction effects on the kinetic energy of quasi-nucleons. The momentum distribution of these quasi-nucleons in the ground state of the system considered is not simply a step function if SRC effects are considered as we discussed in the previous section. Here, we separate the total EDF into a kinetic energy and several potential parts of quasi-nucleons. The $f_J(\mathbf{r}, \mathbf{k})$ and $n_{\mathbf{k}}^J(\rho, \delta)$ with HMTs constrained by the SRC experiments are used in evaluating both the kinetic and the momentum-dependent potential parts of the EDF in ANM at zero temperature. At least for simulating heavy-ion collisions using transport models, how the total EDFs are separated into their kinetic and potential parts are important and have practical consequences in predicting experimental observables [41, 54]. Interestingly, how the SRC may affect the symmetry energy, heavy-ion reactions and properties of neutron stars are among the central issues in our pursuit of understanding the nature of neutron-rich nucleonic matter. Previous attempts to incorporate the experimentally constrained $n_{\mathbf{k}}^J(\rho, \delta)$ and $f_J(\mathbf{r}, \mathbf{k})$ with HMT in the non-relativistic EDF and examine their effects on heavy-ion collisions and neutron stars were found very difficult [55]. This is mainly because of the nontrivial momentum dependence of the $U_J(\rho, \delta, |\mathbf{k}|)$ and the EDF when the SRC-modified $n_{\mathbf{k}}^J(\rho, \delta)$ and $f_J(\mathbf{r}, \mathbf{k})$ are used. Since

one needs to solve 8-coupled equations simultaneously to obtain self-consistently all model parameters from inverting empirical properties of ANM and nucleon optical potentials at ρ_0 , numerical problems associated with the momentum integrals in Eqs. (4) and (8) using the original $\Omega(\mathbf{k}, \mathbf{k}')$ are very difficult to solve.

A new high-momentum regulating function: To avoid the problem mention above, we propose a new high-momentum regulating function $\Omega(\mathbf{k}, \mathbf{k}')$ that approximates very well the original one while enables all integrals in the EDF and $U_J(\rho, \delta, |\mathbf{k}|)$ to be analytically expressed. Perturbatively, if Λ is large compared to the momenta scale in the problems under investigation, the $\Omega(\mathbf{k}, \mathbf{k}')$ in Eq. (7) can be expanded as $\Omega(\mathbf{k}, \mathbf{k}') \approx 1 - \mathbf{k}^2/\Lambda^2 - \mathbf{k}'^2/\Lambda^2 + 2\mathbf{k} \cdot \mathbf{k}'/\Lambda^2$. Using this as a hint, we parameterize the $\Omega(\mathbf{k}, \mathbf{k}')$ as

$$\Omega(\mathbf{k}, \mathbf{k}') = 1 + a \left[\left(\frac{\mathbf{k} \cdot \mathbf{k}'}{\Lambda^2} \right)^2 \right]^{1/4} + b \left[\left(\frac{\mathbf{k} \cdot \mathbf{k}'}{\Lambda^2} \right)^2 \right]^{1/6}, \quad (9)$$

where a and b are two new parameters. It is interesting to note that this $\Omega(\mathbf{k}, \mathbf{k}')$ is invariant under the transformation $a \rightarrow a/\xi^{3/2}$, $b \rightarrow \xi b$ and $\Lambda \rightarrow \Lambda/\xi^{3/2}$, indicating that we have the freedom to first fix one of them without affecting the physical results. Here we set $b = 2$ and then determine the a and Λ using known constraints as we shall discuss in the following.

The advantages of using this new regulating function is twofold: firstly, the basically 1/2 and 1/3 power in the second and third term in (9) is relevant for describing properly the energy dependence of nucleon optical potential [67]; secondly, it enables analytical expressions for the EOS and $U_J(\rho, \delta, |\mathbf{k}|)$ in ANM. We notice that the Ω function is only perturbatively effective at momenta smaller than the momentum scale Λ , indicating that the EDF constructed can only be used to a restricted range of momentum/density. It turns out that the cut-off of the HMT in ANM up to about $3\rho_0$ is significantly smaller than the Λ parameter we use here. The above non-relativistic GHF-EDF is denoted as abMDI in the following.

TABLE I: Coupling constants used in the three sets (right side) and some empirical properties of asymmetric nucleonic matter used to fix them (left side). $b = 2$ and $\Lambda = 1.6 \text{ GeV}/c$ are used in this work. $K_0 \equiv K_0(\rho_0)$, $M_0^* \equiv M_0^*(\rho_0)$, $L \equiv L(\rho_0)$.

Quantity	Value	Coupling	FFG	HMT-SCGF	HMT-exp
$\rho_0 \text{ (fm}^{-3}\text{)}$	0.16	$A_\ell^0 \text{ (MeV)}$	-578.7397	614.1020	307.4366
$E_0(\rho_0) \text{ (MeV)}$	-16.0	$A_u^0 \text{ (MeV)}$	225.6127	711.5675	1055.4219
M_0^*/M	0.58	$B \text{ (MeV)}$	517.5297	-256.9850	-64.5669
$K_0 \text{ (MeV)}$	230.0	$C_\ell \text{ (MeV)}$	-155.6406	-154.2604	-129.5643
$U_0(\rho_0, 0) \text{ (MeV)}$	-100.0	$C_u \text{ (MeV)}$	-285.3256	-351.5893	-587.2980
$E_{\text{sym}}(\rho_0) \text{ (MeV)}$	31.6	σ	1.0353	0.9273	0.6694
$L \text{ (MeV)}$	58.9	a	-5.4511	-5.0144	-4.1835
$U_{\text{sym}}(\rho_0, 1 \text{ GeV}) \text{ (MeV)}$	-20.0	x	0.6144	0.3703	0.1123

We fix all parameters in the model EDF using empirical properties of SNM, ANM and main features of nuclear optical potentials at ρ_0 . More specifically, for SNM we adopt $E_0(\rho_0) = -16$ MeV at the saturation density $\rho_0 = 0.16$ fm $^{-3}$ with $E_0(\rho) = E(\rho, 0)$ the EOS of SNM, its incompressibility $K_0 \equiv [9\rho^2 d^2 E_0(\rho)/d\rho^2]_{\rho_0} = 230$ MeV [56–60], the isoscalar nucleon k-mass, i.e., $M_0^*(\rho)/M = [1 + (M/|\mathbf{k}|)dU_0/d|\mathbf{k}|]_{|\mathbf{k}|=k_F}^{-1}$ [61], is selected as $M_0^*(\rho_0)/M = 0.58$, and $U_0(\rho_0, 0) = -100$ MeV. For the isospin-dependent part in ANM, we adopt $E_{\text{sym}}(\rho_0) = 31.6$ MeV for the symmetry energy, $L \equiv L(\rho_0) = 58.9$ MeV [63] for the slope of the symmetry energy and $U_{\text{sym}}(\rho_0, 1 \text{ GeV}) = -20$ MeV [12] for the symmetry potential, respectively. Moreover, the value of Λ is constrained to fall within a reasonable range to guarantee the effect of the high order terms in δ in the EOS of ANM mainly characterized by the fourth order symmetry energy, i.e., $E_{\text{sym},4}(\rho) \equiv 24^{-1} \partial^4 E(\rho, \delta)/\partial \delta^4|_{\delta=0}$, is smaller than 3 MeV at ρ_0 , to be consistent with predictions of microscopic many-body theories. Consequently, $1.40 \text{ GeV} \lesssim \Lambda \lesssim 1.64 \text{ GeV}$ is obtained and the study based on $\Lambda = 1.6 \text{ GeV}$ is used as the default one. It is worth noting that the single-nucleon potential in SNM thus constructed is consistent with the global relativistic nucleon optical potential extracted from analyzing nucleon-nucleus scattering data [67]. Thus, totally five isoscalar parameters, i.e., $A_t \equiv A_\ell + A_u$, B , $C_t \equiv C_\ell + C_u$, σ and a for SNM, and three isovector parameters, i.e., $A_d \equiv A_\ell - A_u$, $C_d \equiv C_\ell - C_u$ and x are all fixed. Details values of these parameters for the three cases using the same set of input physical properties are shown in Tab. I.

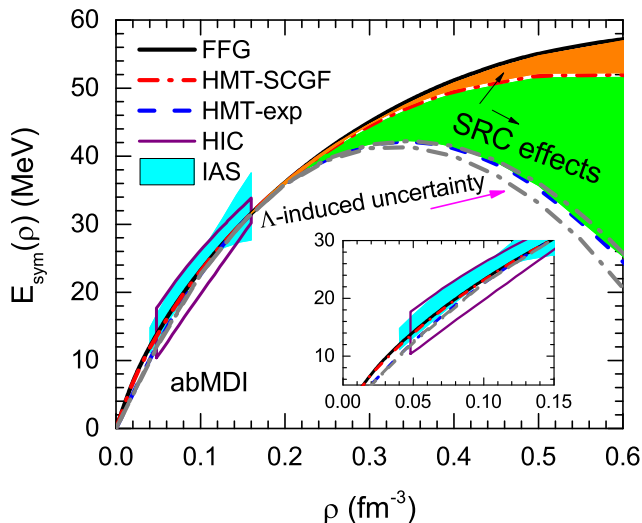


FIG. 1: (Color Online). Density dependence of nuclear symmetry energy $E_{\text{sym}}(\rho)$ using the FFG, HMT-SCGF and HMT-exp parameter set, respectively. Constraints on the symmetry energy from analyzing heavy-ion collisions (HIC) [68] and isobaric analog states (IAS) [69] are also shown for comparisons. The uncertainty range due to the Λ parameter is indicated with the gray dash-dot lines for the HMT-exp set.

Short-range correlation effects on the density dependence of nuclear symmetry energy: Now we turn to effects of the SRC on nuclear symmetry energy. Shown in Fig. 1 are the results obtained using the FFG, HMT-SCGF and HMT-exp parameter sets. By construction, they all have the same $E_{\text{sym}}(\rho_0)$ and L at ρ_0 . Also shown are the constraints on the $E_{\text{sym}}(\rho)$ around ρ_0 from analyzing intermediate energy heavy-ion collisions (HIC) [68] and the isobaric analog states (IAS) [69]. Although the predicted $E_{\text{sym}}(\rho)$ using the three parameter sets can all pass through these constraints, they behave very differently especially at supra-saturation densities. The uncertainty of the $E_{\text{sym}}(\rho)$ due to that of the Λ parameter is also shown in Fig. 1 for the HMT-exp set with the gray dash-dot lines. It is seen that the uncertainty is much smaller than the SRC effect. For example, the variation of the symmetry energy at $3\rho_0$ owing to the uncertainty of Λ is about 2.3 MeV while the SRC effect is about 14.5 MeV. Since the Λ parameter mainly affects the high density/momentum behavior of the EOS, its effects become smaller at lower densities. The reduction of the $E_{\text{sym}}(\rho)$ at both sub-saturation and supra-saturation densities leads to a reduction of the curvature coefficient $K_{\text{sym}} \equiv 9\rho_0^2 d^2 E_{\text{sym}}(\rho)/d\rho^2|_{\rho=\rho_0}$ of the symmetry energy. More quantitatively, we find that the K_{sym} changes from -109 MeV in the FFG set to about -121 MeV and -188 MeV in the HMT-SCGF and HMT-exp set, respectively. It is interesting to stress that this SRC reduction of K_{sym} help reproduce the experimentally measured isospin-dependence of incompressibility $K(\delta) = K_0 + K_\tau \delta^2 + \mathcal{O}(\delta^4)$ in ANM where $K_\tau = K_{\text{sym}} - 6L - J_0 L/K_0$. The skewness of SNM $J_0 \equiv 27\rho_0^3 d^3 E_0(\rho)/d\rho^3|_{\rho=\rho_0}$ is approximately -381 , -376 and -329 MeV in the FFG, HMT-SCGF and HMT-exp set, respectively. The resulting K_τ is found to change from -365 MeV in the FFG set to about -378 MeV and -457 MeV in the HMT-SCGF and HMT-exp set, respectively. The latter is in good agreement with the best estimate of $K_\tau \approx -550 \pm 100$ MeV from analyzing several different kinds of experimental data currently available [60].

It is also interesting to notice that the SRC-induced reduction of $E_{\text{sym}}(\rho)$ within the non-relativistic EDF approach here is qualitatively consistent with the earlier finding within the nonlinear Relativistic Mean-Field (RMF) theory [37]. Nevertheless, since there is no explicit momentum dependence in the RMF EDF, the corresponding reduction of $E_{\text{sym}}(\rho)$ is smaller. Obviously, the momentum-dependent interaction makes the softening of the symmetry energy at supra-saturation densities more evident. This naturally leads us to the question why the SRC reduces the $E_{\text{sym}}(\rho)$ at both sub-saturation and supra-saturation densities. The SRC affects the $E_{\text{sym}}(\rho)$ through several terms. First of all, because of the momentum-squared weighting in calculating the average nucleon kinetic energy, the isospin dependence of the HMT makes the kinetic symmetry energy different from the FFG prediction as already pointed out in several earlier studies [34, 35, 39–41, 70–73]. More specifically, within the parabolic approximation of ANM’s EOS the $E_{\text{sym}}(\rho)$ is approximately the energy difference between PNM and SNM. Thus, the larger HMT due to the stronger SRC dominated by the neutron-proton isosinglet interaction increases signif-

icantly the average energy per nucleon in SNM but has little effect on that in PNM, leading to a reduction of the kinetic symmetry energy. More specifically, the factor Υ_{sym} defined via $E_{\text{sym}}^{\text{kin}}(\rho) = \Upsilon_{\text{sym}} k_{\text{F}}^2 / 6M$ is a measure of the SRC effect on nucleon kinetic energy, and it is determined by the characteristics of n_{k}^J via [35]

$$\begin{aligned} \Upsilon_{\text{sym}} = & 1 + C_0(1 + 3C_1) \left(5\phi_0 + \frac{3}{\phi_0} - 8 \right) \\ & + 3C_0\phi_1 \left(1 + \frac{5}{3}C_1 \right) \left(5\phi_0 - \frac{3}{\phi_0} \right) + \frac{27C_0\phi_1^2}{5\phi_0}. \end{aligned} \quad (10)$$

Numerically, the Υ_{sym} is 0.71 with the HMT-SCGF parameters while it is -1.12 with the HMT-exp parameters consistent with earlier estimates [41]. Of course, the HMT also affects the momentum dependent part of the potential symmetry energy. However, the strength parameters C_u and C_ℓ are not independently determined but through the global optimization of the EDF. The reduction of the kinetic symmetry energy is naturally compensated by the increased potential contribution in optimizing the EDF to keep the $E_{\text{sym}}(\rho_0)$ and L consistent with empirical constraints at ρ_0 [63]. However, because of the $\rho^{2/3}$ dependence of the kinetic symmetry energy, after readjusting the model parameters in the global optimization process using empirical properties of ANM and SNM at ρ_0 , the reduction of kinetic $E_{\text{sym}}(\rho)$ still dominates over the increase of potential symmetry energy at abnormal densities, leading to the overall reduction of $E_{\text{sym}}(\rho)$ at both sub-saturation and supra-saturation densities.

Implications of the SRC-modified $E_{\text{sym}}(\rho)$ on properties of neutron stars: The SRC-modified EOS and single-particle potentials are expected to affect properties of both heavy-ion collisions and neutron stars. While investigations of explicit SRC effects on experimental observables are currently underway, we present here SRC effects on two internal properties of neutron stars that may have consequences on observables. Firstly, the pressure of neutron-rich nucleonic matter around ρ_0 can be written as

$$\begin{aligned} p/3\rho & \approx L(\rho)\delta^2 + 3\rho \frac{dE_0(\rho)}{d\rho} \\ & \approx L\delta^2 \left(1 + 3\chi + \frac{9}{2}\chi^2 \right) + K_0\chi(1 + 3\chi) \\ & + \chi \left[\frac{1}{2}\chi J_0 + K_{\text{sym}}\delta^2(1 + 3\chi) \right] \end{aligned} \quad (11)$$

where $\chi = (\rho - \rho_0)/3\rho_0$. Near ρ_0 , it is well known that the pressure is dominated by the $L\delta^2$ term. Keeping the K_0 and L the same by design in our study here, effects of the SRC on the pressure is through the decrease of K_{sym} and increase of J_0 as we discussed earlier. The overall effect, however, depends on the density χ and isospin asymmetry δ . For example, comparing the HMT-exp with the FFG model calculations, the increase in J_0 is $\Delta J_0 \equiv J_0^{\text{HMT-exp}} - J_0^{\text{FFG}} = 52$ MeV and the decrease in K_{sym} is $\Delta K_{\text{sym}} \equiv K_{\text{sym}}^{\text{HMT-exp}} - K_{\text{sym}}^{\text{FFG}} = -79$ MeV. For very neutron-rich matter in neutron stars with $\delta \geq 0.5$, the

decrease in K_{sym} dominates, leading to an appreciable softening of the EOS. While for much smaller values of δ , such as the average isospin asymmetry in ^{208}Pb or those normally reached in heavy-ion reactions, the SRC effect on pressure is small when the K_0 and L are kept constants. The latter two quantities are known to affect the maximum masses and radii of neutron stars. We thus expect the SRC to have some effects on the mass-radius correlation of neutron stars. However, the results will depend on our choice for the K_0 and L as we shall report elsewhere [74].

Many interesting microphysics in neutron stars depend critically on the proton fraction x_p at β -equilibrium. The latter is uniquely determined by the nuclear symmetry energy. For neutrino free β -stable matter, the chemical equilibrium for the npe μ matter requires $\mu_e = \mu_\mu = \mu_n - \mu_p = 4E_{\text{sym}}(\rho)\delta + 8E_{\text{sym},4}(\rho)\delta^3 + \dots \approx 4E_{\text{sym}}(\rho)\delta + 8E_{\text{HO}}(\rho)\delta^3$ with μ 's the respective chemical potentials of particles involved. Moreover, the $E_{\text{HO}}(\rho) = E_{\text{sym},4}(\rho) + E_{\text{sym},6}(\rho) + \dots = E_{\text{PNM}}(\rho) - E_0(\rho) - E_{\text{sym}}(\rho)$ denotes the high-order δ effect of the ANM's EOS, where $E_{\text{PNM}}(\rho)$ is the EOS of PNM. Then $x_p = \rho_p/\rho = x_e + x_\mu$ because of charge neutrality. Shown in Fig. 2 are the proton fractions x_p in the npe μ matter as a function of density obtained using the three sets of model parameters in both the parabolic approximation and the one including the high-order term $E_{\text{HO}}(\rho)$, respectively. It is seen that the high-order term $E_{\text{HO}}(\rho)$ plays a significant role at supra-saturation densities especially in the HMT-exp case. Although we have restricted the quartic symmetry energy at ρ_0 to be less than 3 MeV in the optimization of the model EDF, it is clear that the SRC induces a significant $E_{\text{HO}}(\rho)$ at supra-saturation densities. This is understandable as we have shown earlier analytically that the SRC-induced isospin dependence of the HMT leads to a significant quartic term in the kinetic symmetry energy [35].

The critical proton fraction $x_p \approx 14\%$ (11%) for the direct URCA process to occur in npe μ (npe) matter assuming nucleons have the FFG momentum distribution is also shown in Fig. 2. It was predicted a long time ago that the threshold x_p value for the direct URCA is reduced by the SRC [75]. However, how the neutrino emissivity near the threshold may be affected by the SRC has not been worked out consistently yet [76]. We notice by passing that so far there is no confirmed observation of direct URCA in any neutron star although it has been predicted to occur by many models [77]. Obviously, more work on this issue remains to be done. Nevertheless, it is interesting to note that the x_p obtained in the HMT-exp starts to decrease at about $2.5\rho_0$ with a maximum proton fraction $x_p \approx 9.6\%$. On the other hand, with both the FFG and HMT-SCGF parameters, the x_p continues to increase to high densities. If the conventional estimates for the direct URCA thresholds remain valid, the FFG and HMT-SCGF would allow while the HMT-exp would forbid the direct URCA process in neutron stars.

Another interesting quantity depends critically on the $E_{\text{sym}}(\rho)$ is the transition density ρ_t , which separates the liquid core from the inner crust in neutron stars. It depends sensitively on the low-density behavior of $E_{\text{sym}}(\rho)$ and plays an important role in determining many properties of neutron

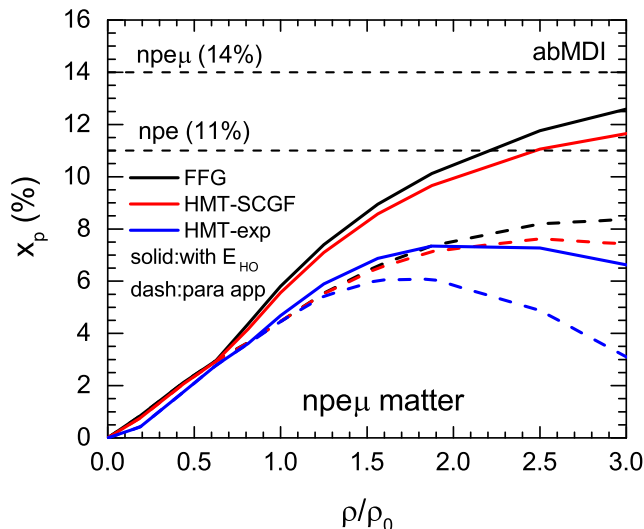


FIG. 2: (Color Online). The proton fraction x_p in $npe\mu$ matter as a function of density with or without considering the high-order effects in the EOS of ANM using the FFG, HMT-exp and HMT-SCGF parameter set, respectively.

stars, such as the fractional moment of inertia of the crust relevant for understanding the glitch phenomenon [9, 78–82]. One simple and widely used approach to determine the ρ_t is to examine when the following stability condition is violated [9, 83]

$$\mathcal{U}_{\text{th}} = 2\rho \frac{\partial E(\rho, x_p)}{\partial \rho} + \rho^2 \frac{\partial^2 E(\rho, x_p)}{\partial \rho^2} - \left(\frac{\partial^2 E(\rho, x_p)}{\partial \rho \partial x_p} \rho \right)^2 \bigg/ \frac{\partial^2 E(\rho, x_p)}{\partial x_p^2} > 0. \quad (12)$$

Here, the $E(\rho, x_p)$ is the energy per nucleon in β -equilibrium npe matter (the core-crust transition occurs at low densities where muons generally do not appear), see, e.g., (4), and the pressure $p = p_N + p_e$ has contributions from both nucleons (p_N) and electrons (p_e). The ρ_t is found to be about 0.069, 0.062 and 0.030 fm^{-3} for the FFG, HMT-SCGF and HMT-exp case, respectively. The corresponding transition pressure is found to be about 0.38, 0.30 and 0.07 MeV/fm^3 , respectively. The Λ parameter is found to have very small effects on the transition density ρ_t and pressure p_t . It is interesting to see

that the SRC brings significant changes to the transition density and pressure. For example, compared to the FFG case, the ρ_t in the HMT-exp calculation is reduced by about 57%.

The above discussions about effects of the SRC-modified $E_{\text{sym}}(\rho)$ on microphysics happening in neutron stars may help establish a connection between the SRC and astrophysical observations. In addition, the SRC-modified single-nucleon potential and EOS of ANM can be used directly in transport model simulations of nuclear reactions, providing a link between the SRC and observables in terrestrial experiments. Explorations of these links and comparisons with data will help us better understand the underlying physics determining the elusive nature of neutron-rich nucleonic matter.

Summary: Within a modified non-relativistic GHF-EDF approach and using a new momentum regulating function, we studied effects of SRC-induced HMT in the single-nucleon momentum distribution on the density dependence of nuclear symmetry energy. After re-optimizing the modified GHF-EDF by reproducing the same empirical properties of ANM, SNM and major features of nucleon optical potential at saturation density, the $E_{\text{sym}}(\rho)$ was found to decrease at both sub-saturation and supra-saturation densities, leading to a reduced curvature K_{sym} of $E_{\text{sym}}(\rho)$ and subsequently a smaller K_τ for the isospin-dependence of nuclear incompressibility in better agreement with its experimental value. Astrophysical implications of this finding were also discussed. In particular, the proton fraction as well as the core-crust transition density and pressure in neutron stars at β equilibrium are found to decrease as the fraction of HMT nucleons in SNM increases, linking clearly properties of neutrons stars with the microphysics of SRC. Moreover, the SRC-modified EOS and the single-nucleon potentials in ANM can be used in future transport model simulations of heavy-ion collisions to investigate SRC effects in dense neutron-rich matter in terrestrial laboratories.

Acknowledgement: We would like to thank L.W. Chen, O. Hen and E. Piasezky for helpful discussions. This work was supported in part by the U.S. Department of Energy, Office of Science, under Award Number DE-SC0013702, the CUSTIPEN (China-U.S. Theory Institute for Physics with Exotic Nuclei) under the US Department of Energy Grant No. DE-SC0009971 and the National Natural Science Foundation of China under Grant No. 11320101004.

[1] J. Decharge and D. Gogny, Phys. Rev. C **21**, 1568 (1980).
 [2] C. Gale, G. Bertsch, and S. Das Gupta, Phys. Rev. C **35**, 1666 (1987).
 [3] M. Prakash, T. T. S. Kuo and S. Das Gupta, Phys. Rev. C **37**, 2253 (1988).
 [4] G. M. Welke, M. Prakash, T. T. S. Kuo, S. Das Gupta and C. Gale, Phys. Rev. C **38**, 2101 (1988).
 [5] C. Gale, G. M. Welke, M. Prakash, S. J. Lee and S. Das Gupta, Phys. Rev. C **41**, 1545 (1990).

[6] Q. Pan and P. Danielewicz, Phys. Rev. Lett. **70**, 2062 (1993); **70**, 3523 (1993).
 [7] J. Zhang, S. Das Gupta and C. Gale, Phys. Rev. C **50**, 1617 (1994).
 [8] V. K. Mishra, G. Fai, L. P. Csernai, and E. Osnes, Phys. Rev. C **47**, 1519 (1993).
 [9] J. Xu, L.W. Chen, B.A. Li, and H.R. Ma, Phys. Rev. C **79**, 035802 (2009); Astrophys. J. **697**, 1549 (2009).
 [10] B. Behera, T.R. Routray, and S.K. Tripathy, J. Phys. G: Nucl.

- Part. Phys. **38**, 115104 (2011).
- [11] C. Constantinou, B. Muccioli, M. Prakash and J. M. Lattimer, Phys. Rev. C **92**, 025801 (2015).
- [12] J. Xu, L.W. Chen, and B.A. Li, Phys. Rev. C **91**, 014611 (2015).
- [13] I. Bombaci in *Isospin Physics in Heavy-Ion Collisions at Intermediate Energies*, eds. Bao-An Li and W. Udo Schroder (Nova Science Publishers, Inc., New York, 2001), p.35
- [14] C.B. Das, S. Das Gupta, C. Gale, and B.A. Li, Phys. Rev. C **67** (2003) 034611
- [15] C. Xu and B.A. Li, Phys. Rev. C **81**, 044603 (2010).
- [16] B.A. Li, C. B. Das, S. Das Gupta, C. Gale, Phys. Rev. C **69** (2004) 011603 (R); Nucl. Phys. A **735** (2004) 563.
- [17] L.W. Chen, C.M. Ko, B.A. Li, C. Xu, and J. Xu, Eur. Phys. J. A **50**, 29 (2014).
- [18] L.W. Chen, C.M. Ko, B.A. Li, and G.C. Yong, Front. Phys. China **2**, 327 (2007).
- [19] B.A. Li, L.W. Chen, and C.M. Ko, Phys. Rep. **464**, 113 (2008).
- [20] M.D. Cozma, Phys. Lett. **B700**, 139 (2011).
- [21] “Topical issue on nuclear symmetry energy”, Eds., B.A. Li, A. Ramos, G. Verde, and I. Vidaña, Eur. Phys. J. A **50**, 9, (2014).
- [22] H.A. Bethe, Ann. Rev. Nucl. Part. Sci. **21**, 93 (1971).
- [23] A.N. Antonov, P.E. Hodgson, and I.Zh. Petkov, *Nucleon Momentum and Density Distribution in Nuclei*, Clarendon Press, Oxford, 1988.
- [24] J. Arrington, D.W. Higinbotham, G. Rosner, and M. Sargsian, Prog. Part. Nucl. Phys. **67**, 898 (2012).
- [25] C. Ciofi degli Atti, Phys. Rep. **590**, 1 (2015).
- [26] Jan Ryckebusch, Maarten Vanhalst and Wim Cosyn, Journal of Physics G: Particles and Nuclei **42**, 055104 (2015).
- [27] O. Hen, G.A. Miller, E. Piasezky, and L.B. Weinstein, arXiv:1611.09748, Review of Modern Physics (2017) in press.
- [28] R. Weiss, B. Bazak, and N. Barnea, Phys. Rev. Lett. **114**, 012501 (2015).
- [29] R. Weiss, B. Bazak, and N. Barnea, Phys. Rev. C **92**, 054311 (2015).
- [30] O. Hen *et al.*, Science **346**, 614 (2015).
- [31] O. Hen, L.B. Weinstein, E. Piasezky, G.A. Miller, M. Sargsian, and Y. Sagi, Phys. Rev. C **92**, 045205 (2015).
- [32] C. Colle, O. Hen, W. Cosyn, I. Korover, E. Piasezky, J. Ryckebusch, and L.B. Weinstein, Phys. Rev. C **92**, 024604 (2015).
- [33] K.S. Egiyan *et al.*, Phys. Rev. Lett. **96**, 082501 (2006); E. Piasezky *et al.*, Phys. Rev. Lett. **97**, 162504 (2006); R. Shneur *et al.*, Phys. Rev. Lett. **99**, 072501 (2007); R. Subedi *et al.*, Science **320**, 1467 (2008); L.B. Weinstein *et al.*, Phys. Rev. Lett. **106**, 052301 (2011); I. Korover *et al.*, Phys. Rev. Lett. **113**, 022501 (2014).
- [34] A. Rios, A. Polls, and W.H. Dickhoff, Phys. Rev. C **79**, 064308 (2009); *ibid* C **89**, 044303 (2014).
- [35] B.J. Cai and B.A. Li, Phys. Rev. C **92**, 011601(R) (2015).
- [36] B.J. Cai and B.A. Li, Phys. Lett. **B759**, 79 (2016).
- [37] B.J. Cai and B.A. Li, Phys. Rev. C **93**, 014619 (2016).
- [38] B.J. Cai, B.A. Li, and L.W. Chen, Phys. Rev. C **94**, 061302(R) (2016)
- [39] C. Xu and B.A. Li, arXiv:1104.2075.
- [40] C. Xu, A. Li, B.A. Li, J. of Phys: Conference Series **420**, 012190 (2013).
- [41] O. Hen, B.A. Li, W.J. Guo, L.B. Weinstein, and E. Piasezky, Phys. Rev. C **91**, 025803 (2015).
- [42] O. Hen, A. Steiner, E. Piasezky, and L. Weinstein, arXiv:1608.00487.
- [43] P. Yin, J.Y. Li, P. Wang, and W. Zuo, Phys. Rev. C **87**, 014314 (2013).
- [44] Z.H. Li and H.J. Schulze, Phys. Rev. C **94**, 024322 (2016),
- [45] S.N. Tan, Ann. Phys. **323**, 2952 (2008); **323**, 2971 (2008); **323**, 2987 (2008).
- [46] E. Braaten, D. Kang, and L. Platter, Phys. Rev. Lett. **106**, 153005 (2011).
- [47] F. Werner and Y. Castin, Phys. Rev. A **86**, 053633 (2012).
- [48] D.H. Smith, E. Braaten, D. Kang, and L. Platter, Phys. Rev. Lett. **112**, 110402 (2014).
- [49] P. Makotyn *et al.*, Nat. Phys. **10**, 116 (2014).
- [50] R.J. Fletcher *et al.*, Science **355**, 377 (2017).
- [51] L.W. Chen, C.M. Ko, and B.A. Li, Phys. Rev. Lett. **94**, 032701 (2005).
- [52] G. F. Bertsch and S. Das Gupta, Phys. Rep. **160**, 189 (1988).
- [53] J. Aichelin, Phys. Rep. **202**, 233 (1991).
- [54] B.A. Li, W.J. Guo and Z.Z. Shi, Phys. Rev. C **91**, 044601 (2015).
- [55] X.H. Li and W.J. Guo, private communications.
- [56] D.H. Youngblood, H.L. Clark, and Y.-W. Lui, Phys. Rev. Lett. **82**, 691 (1999).
- [57] S. Shlomo, V.M. Kolomietz, and G. Colò, Eur. Phys. J. A **30**, 23 (2006).
- [58] J. Piekarewicz, J. Phys. G **37**, 064038 (2010).
- [59] L.W. Chen and J.Z. Gu, J. Phys. G **39**, 035104 (2012).
- [60] G. Colò, U. Garg and H. Sagawa, Eur. Phys. J. A **50**, 26 (2014).
- [61] B.A. Li and L.W. Chen, Mod. Phys. Lett. A **30**, 1530010 (2015).
- [62] B.A. Li, B.J. Cai, L.W. Chen, and X.H. Li, Nucl. Sci. Tech. **27**, 141 (2016).
- [63] B.A. Li and X. Han, Phys. Lett. **B727**, 276 (2013).
- [64] J. Xu and C.M. Ko, Phys. Rev. C **82**, 044311 (2010).
- [65] C. Xu, B.A. Li, and L.W. Chen, Phys. Rev. C **82**, 054607 (2010).
- [66] C. Xu, B.A. Li, L.W. Chen, and C.M. Ko, Nucl. Phys. **A865**, 1 (2011).
- [67] S. Hama, B.C. Clark, E.D. Cooper, H.S. Sherif, and R.L. Mercer, Phys. Rev. C **41**, 2737 (1990).
- [68] B.M. Tsang *et al.*, Phys. Rev. C **86**, 105803 (2012).
- [69] P. Danielewicz and J. Lee, Nucl. Phys. **A922**, 1 (2014).
- [70] I. Vidaña, A. Polls, and C. Providência, Phys. Rev. C **84**, 062801(R) (2011).
- [71] A. Lovato, O. Benhar, S. Fantoni, A.Yu. Illarionov, and K.E. Schmidt, Phys. Rev. C **83**, 054003 (2011).
- [72] A. Carbone, A. Polls, A. Rios, Eur. Phys. Lett. **97**, 22001 (2012).
- [73] A. Carbone, A. Polls, C. Providência, A. Rios, and I. Vidaña, Eur. Phys. A **50**, 13 (2014).
- [74] B.J. Cai and B.A. Li, in preparation.
- [75] L. Frankfurt, M. Sargsian, and M. Strikman, Int. Jour. Mod. Phys. A **23**, 2991 (2008).
- [76] I. Vidana and W.G. Newton, private communications.
- [77] A. Y. Potekhin, J. A. Pons and Dany Page, Space Sci. Rev. **191**, 239 (2015).
- [78] C.J. Horowitz and J. Piekarewicz, Phys. Rev. Lett. **86**, 5647 (2001).
- [79] C. Providência, L. Brito, S.S. Avancini, D.P. Menezes, and P. Chomaz, Phys. Rev. C **73**, 025805 (2006).
- [80] C. Ducoin, J. Margueron, and P. Chomaz, Nucl. Phys. **A809**, 30 (2008).
- [81] C. Ducoin, C. Providência, A.M. Santos, L. Brito, and P. Chomaz, Phys. Rev. C **78**, 055801 (2008).
- [82] J.M. Lattimer and M. Prakash, Phys. Rep. **442**, 109 (2007).
- [83] S. Kubis, Phys. Rev. C **76**, 035801 (2007); Phys. Rev. C **70**, 065804 (2004).